

MLVTG: Mamba-Based Feature Alignment and LLM-Driven Purification for Multi-Modal Video Temporal Grounding

Zhiyi Zhu¹, Xiaoyu Wu¹, Zihao Liu¹, and Linlin Yang¹

Communication University of China, Beijing 100020, China
 {zhuzhiyi,wuxiaoyu,liuzihao}@cuc.edu.cn, mu4yang@gmail.com

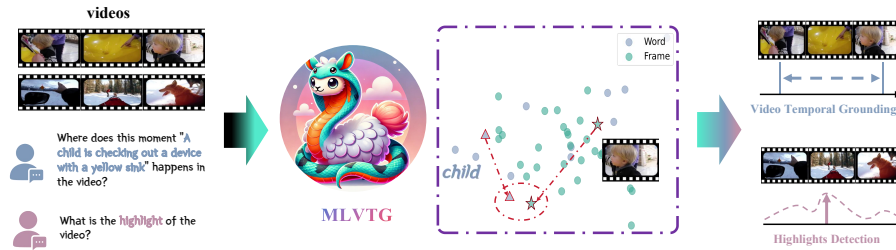


Fig. 1: **MLVTG** projects features of video-text pairs into a shared semantic space, narrows the semantic gap, and better aligns visual-text features. Its dual-branch architecture handles temporal localization and highlight detection separately, allowing task-specific optimization.

Abstract. Video Temporal Grounding (VTG), which aims to localize video clips corresponding to natural language queries, is a fundamental yet challenging task in video understanding. Existing Transformer-based methods often suffer from redundant attention and suboptimal multi-modal alignment. To address these limitations, we propose MLVTG, a novel framework that integrates two key modules: MambaAligner and LLMRefiner. MambaAligner uses stacked Vision Mamba blocks as a backbone instead of Transformers to model temporal dependencies and extract robust video representations for multi-modal alignment. LLMRefiner leverages the specific frozen layer of a pre-trained Large Language Model (LLM) to implicitly transfer semantic priors, enhancing multi-modal alignment without fine-tuning. This dual alignment strategy, temporal modeling via structured state-space dynamics and semantic purification via textual priors, enables more precise localization. Extensive experiments on QVHighlights, Charades-STA, and TVSum demonstrate that MLVTG achieves state-of-the-art performance and significantly outperforms existing baselines.

Keywords: Video Temporal Grounding · Mamba · Large Language Model

1 Introduction

In video understanding research, untrimmed videos dominate digital content yet contain sparse valuable clips, creating critical demand for Video Temporal Grounding (VTG) - the task of aligning queries with precise temporal localization in untrimmed videos. Researchers consider that its fundamental capability covers two key tasks: Temporal Localization (TL) and Highlight Detection (HD). However, effectively executing these tasks presents significant challenges. Current limitations stem from inherent modality discrepancies in multi-modal alignment, where heterogeneous representations of visual dynamics and linguistic structures create matching ambiguities that degrade system performance [23]. Addressing these challenges could revolutionize human-AI video interaction, enabling real-time applications.

Early methods rely on 3D CNNs [9, 14, 7, 19], but limit receptive fields resulted in insufficient video representation capability, leading to coarse multi-modal alignment. Transformer-based models [4, 18, 26, 23], leveraging the attention mechanism, have advanced VTG by effectively capturing global contextual dependencies. However, Transformers often suffer from redundant attention across frames [42, 3, 1], weakening temporal discrimination. Recently, state space models (SSMs) based Mamba [11] have demonstrated strong sequence modeling capacity in vision tasks [25, 46] by dynamically filtering redundant signals. Yet, directly applying Mamba to VTG lacks temporal expressiveness. To address this, we adopt the bidirectional scanning strategy from [20, 46], stacking multiple Vision Mamba blocks to extract robust video representations for multi-modal alignment.

To ensure that video temporal modeling possesses stronger semantic expressiveness and accuracy, we further introduce large language mode (LLM) to enhance multi-modal alignment. It exhibits strong multi-modal reasoning abilities [34, 6, 41], effectively suppressing noise, purifying semantics and enhancing multi-modal alignment in video tasks [45, 5]. To leverage such capabilities, we utilize the specific frozen layer of pre-trained LLMs. With frozen pre-trained parameters, LLMs can transfer textual priors to visual domains, filtering redundant video content. According to the Platonic Representation Hypothesis [17], neural networks converge to a shared semantic space across modalities, allowing LLMs to associate abstract textual concepts (e.g., “running”) with temporal visual patterns (e.g., “leg movement”), thereby improving alignment and robustness.

Overall, we propose Mamba-based feature alignment and LLM-driven purification for multi-modal Video Temporal Grounding termed MLVTG, a novel framework that combines MambaAligner and mamba-based LLMRefiner. MLVTG features a dual-branch alignment strategy: structured SSM enables adaptive feature selection, while a frozen LLM layer performs semantic purification. By replacing the Transformer with vision mamba blocks, our model reduces redundant attention, enhances temporal modeling, and aligns multi-modality. The SSM branch captures salient video context via selective memory, and the LLM-Refiner projects high-level semantics without fine-tuning. MLVTG is the first

to jointly leverage Mamba and LLM for VTG, achieving SOTA results on three benchmarks. Our key contributions are:

- We propose MLVTG, a novel dual-branch architecture that handles temporal localization and highlight detection separately, allowing task-specific optimization.
- We propose the MambaAligner, a stack of vision mamba blocks that replaces Transformer to better capture video representations and enhance multi-modal alignment.
- We introduce the mamba-based LLMRefiner, which uses the specific frozen LLM layer to purify semantics through implicit multi-modal interactions without fine-tuning.
- Experiments on QVHighlights, Charades-STA, and TVSum show that our method MLVTG outperforms baseline and achieves state-of-the-art results.

2 Related Work

2.1 Video Temporal Grounding

Video Temporal Grounding (VTG), a key task linking visual content with semantics, has evolved into two sub-tasks: Temporal Localization (TL) and Highlight Detection (HD). TL focuses on grounding natural language queries to video clips, with early proposal-based methods [9, 14] suffering from low coverage, while proposal-free models [19, 44] improve efficiency via direct boundary regression. HD, in contrast, identifies salient video moments, progressing from ranking-based methods [13] to DETR-based detectors [26] with improved accuracy. Though traditionally studied separately, TL and HD share temporal reasoning goals. M-DETR [18] unified them using QVHighlights, inspiring subsequent work on audio integration [24], negative sample learning, and multi-task setups [36]. However, existing methods still struggle with fine-grained multi-modal alignment. To this end, we introduce MLVTG, which jointly optimizes low-level temporal structure by MambaAligner and high-level semantics by LLMRefiner, achieving improvements in both TL and HD tasks.

2.2 Mamba for Sequence Tasks

State Space Models (SSMs) represent long-range sequences with linear complexity [11, 12], offering an efficient alternative to Transformers by leveraging continuous state representations. However, traditional SSMs lack the ability to dynamically focus on task-relevant features across varying contexts. To address this, Mamba [10] introduces gated selective SSMs, improving both noise suppression and salient temporal pattern extraction.

Originally surpassing Transformers in language modeling and time-series forecasting [10, 8, 22], Mamba has recently been extended to vision task [46, 29] and video understanding [20, 27, 25]. However, existing Mamba-based models primarily focus on unimodal tasks and overlook fine-grained video-language

alignment. To overcome this, we incorporate a bidirectional SSM mechanism inspired by VideoMamba, and stack multiple Vision Mamba blocks to capture robust video representations. This enables precise localization for VTG tasks by enhancing temporal modeling and multi-modal alignment.

2.3 Large Language Model for Video Temporal Grounding

Applying Large Language Models (LLMs) to VTG has become a focus of recent research, with several studies exploring different integration strategies. For example, VTimeLLM [16] employs LLM as the VTG decoder to directly output start and end timestamps. However, these existing methods face significant challenges, including limited capabilities in fine-grained temporal reasoning and precise timestamp localization inherent to current LLM architectures. Additionally, the requirement for extensive training exacerbates computational overhead. Motivated by [28], we propose the mamba-based LLMRefiner, a module that efficiently exploits semantic priors embedded within the specific frozen LLM layer. This strategy achieves enhanced semantic alignment between linguistic concepts and corresponding video clips, thereby significantly improving VTG performance.

3 Methodology

3.1 Problem Definition

VTG aims to align natural language descriptions with corresponding moments in untrimmed videos. It covers two major tasks: Temporal Localization and Highlight Detection, both requiring effective multi-modal reasoning.

Temporal Localization. Given a video $\{f_t\}_{t=1}^T$ with frames $f_t \in \mathbb{R}^{H \times W \times 3}$, and a language query $\{q_i\}_{i=1}^{L_q}$, the goal is to predict a temporal clip $\tau = [\tau_s, \tau_e]$ that best matches the query. The core challenge lies in fine-grained multi-modal alignment. A model $F_\theta(\{f_t\}_{t=1}^T, \{q_i\}_{i=1}^{L_q})$ is trained to output $\hat{\tau}$ such that $\text{IoU}(\hat{\tau}, \tau_{\text{gt}}) \geq \alpha$, where $\alpha = 0.5$ is the standard threshold.

Highlight Detection. Given a video $\{f_t\}_{t=1}^T$, the objective is to assign a saliency score s_i to each temporal clip v_i and select the top- K clips with the highest scores as highlights. Formally, the output is the set $M = \{f_i \mid s_i \in \text{top-}K\}$. In scenarios lacking explicit annotations, weak supervision signals such as video titles or domain labels can guide model training. [30, 32]

3.2 Overall Framework – MLVTG

As illustrated in Fig.2, MLVTG integrates the MambaAligner with LLMRefiner, optimizing a multi-modal feature alignment mechanism. Through a dual-branch decoupled task architecture, collaborative reasoning optimization is achieved for temporal localization and highlight detection.

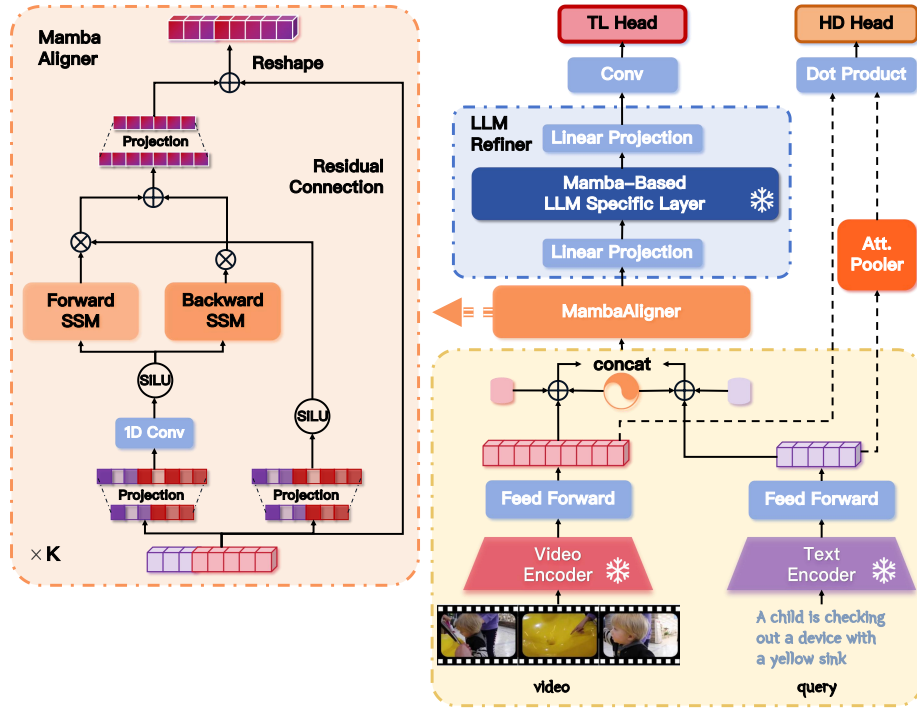


Fig. 2: **Overview of the MLVTG Framework.** The input video and query are first encoded by frozen feature encoders, then projected into a shared semantic space via FFN (Sec. 3.2). One branch computes saliency scores directly, while the other processes concatenated features through the **MambaAligner** (Sec. 3.2), where bidirectional 1D convolutions and SiLU-activated recurrent SSMs dynamically filter spatiotemporal features via selective memory. The aligned features undergo semantic purification through mamba-based **LLMRefiner** (Sec. 3.2), leveraging implicit multi-modal correlations to align modalities while preserving task-relevant semantics. Finally, task-specific heads (Sec. 3.2) classify the optimized features to produce grounding results.

Feature Extraction and Projection. Given an input video with L_v clips and a text query with L_q tokens, we follow the encoder design of [23] to extract features, which are then projected into a shared D -dimensional space via separate Feed-Forward Networks. This yields video features $\mathbf{V} = \{\mathbf{v}_i\}_{i=1}^{L_v} \in \mathbb{R}^{L_v \times D}$ and text features $\mathbf{Q} = \{\mathbf{q}_j\}_{j=1}^{L_q} \in \mathbb{R}^{L_q \times D}$.

We propose a dual branch task decoupled architecture. In the one branch, an attentive pooling mechanism aggregates query tokens $\mathbf{Q} \in \mathbb{R}^{L_q \times D}$ into a sentence-level representation $\mathbf{S} \in \mathbb{R}^{1 \times D}$ to compute a saliency score via similarity measurement:

$$\mathbf{S} = \mathbf{M}\mathbf{Q}, \quad \mathbf{M} = \text{Softmax}(\mathbf{W}\mathbf{Q}) \in \mathbb{R}^{1 \times L_q}, \quad (1)$$

where $\mathbf{W} \in \mathbb{R}^{1 \times L_q}$ is a learnable embedding. In another branch, we incorporate positional embeddings \mathbf{E}^{pos} and modality-type embeddings \mathbf{E}^{type} into both video and query tokens to preserve spatial and modality distinctions:

$$\tilde{\mathbf{V}} = \mathbf{V} + \mathbf{E}_V^{pos} + \mathbf{E}_V^{type}, \quad \tilde{\mathbf{Q}} = \mathbf{Q} + \mathbf{E}_T^{pos} + \mathbf{E}_T^{type}. \quad (2)$$

These representations are concatenated as $\mathbf{Z} = [\tilde{\mathbf{Q}}; \tilde{\mathbf{V}}] \in \mathbb{R}^{L \times D}$, where $L = L_q + L_v$. Subsequently, \mathbf{Z} passes through MambaAligner for robust video representations and multi-modal alignment.

MambaAligner. To better capture video representations for multi-modal alignment, MambaAligner consists of K stacked vision mamba blocks and takes the concatenated feature sequence $\mathbf{Z} = [\tilde{\mathbf{Q}}; \tilde{\mathbf{V}}]$ as the input (see Fig. 2). The input is first normalized and projected into two branches:

$$\hat{\mathbf{Z}} = \text{Norm}(\mathbf{Z}), \quad \mathbf{x} = W_x \hat{\mathbf{Z}}, \quad \mathbf{g} = W_g \hat{\mathbf{Z}}, \quad (3)$$

where Norm denotes layer normalization, and W_x, W_g are learnable projections. Here, \mathbf{x} is used for sequence modeling, while \mathbf{g} serves as the gating signal.

A 1D convolution layer extracts local features from \mathbf{x} , generating forward and backward sequences \mathbf{x}^f and \mathbf{x}^b , respectively. Each is passed through a SSM with parameters (A, B, C) :

$$\mathbf{y} = \mathbf{x} * \mathbf{K}, \quad \mathbf{K} = [CA^0B, CA^1B, \dots, CA^{L-1}B], \quad (4)$$

where \mathbf{K} is the impulse response kernel and $*$ denotes convolution. This yields \mathbf{y}^f and \mathbf{y}^b , capturing global context in both directions.

To fuse the outputs, a gating mechanism uses the control signal \mathbf{g} :

$$\mathbf{y}_{\text{fused}} = \sigma(\mathbf{g}) \odot \mathbf{y}^f + (1 - \sigma(\mathbf{g})) \odot \mathbf{y}^b, \quad (5)$$

where $\sigma(\cdot)$ is the SiLU activation, and \odot denotes element-wise multiplication. The final output is computed via residual connection:

$$\mathbf{Z}_{\text{out}} = \mathbf{Z} + \mathbf{y}_{\text{fused}}.$$

LLMRefiner. To refine the semantics of latent representations and enhance multi-modal alignment, we propose the mamba-based LLMRefiner module. This module integrates two linear layers, denoted as F_L^1 and F_L^2 , along with a pre-trained mamba-based large language model layer (F_{LLM}). Recent studies have highlighted the robust multi-modal reasoning abilities inherent to LLM, demonstrating their effectiveness in noise suppression and semantic refinement. Leveraging these inherent capabilities, our approach utilizes a specific frozen layer from pre-trained LLM. This mamba-based layer, F_{LLM} , operates with frozen parameters to transfer textual priors effectively into the visual domain, thereby filtering out redundant or irrelevant video content.

Due to the dimension mismatch between the output of the MambaAligner(\mathbf{Z}_{out}), and the input dimension requirements of the F_{LLM} layer, we integrate linear projection layers F_L^1 and F_L^2 before and after the F_{LLM} block, respectively. These projection layers harmonize the dimensional compatibility, modifying the network output according to the following formulation:

$$\mathbf{Z}_{refine} = F_L^1 * F_{LLM}(\mathbf{Z}_{out}) * F_L^2. \quad (6)$$

In our implementation, the parameters of the pre-trained F_{LLM} block remain entirely frozen to preserve their robust semantic representation capability. In contrast, the linear projection layers, F_L^1 and F_L^2 , are fully trainable and optimized throughout the training process. This targeted training approach ensures continuous refinement of semantic alignment specifically tailored for downstream multi-modal alignment tasks.

Joint Optimization for TL & HD. To jointly solve TL and HD, we design a dual-head module to produce task-specific outputs coupled with corresponding optimization objectives. Specifically, the TL Head takes refined feature \mathbf{Z}_{refine} as input and integrates two parallel parts composed of 1D conv layers. One predicts the start and end timestamps ($[st, ed]$), while the other performs frame-level binary classification to discriminate foreground from background frames. In contrast, the HD Head receives video features \mathbf{V} and sentence-level representations \mathbf{S} as input and focuses on frame-level salient scores. The overall training objective aggregates task-specific losses with balancing coefficients, formulated as follows:

$$\begin{aligned} \mathcal{L}_{overall} &= \mathcal{L}_{TL} + \mathcal{L}_{HD} \\ &= \lambda_f \mathcal{L}_f + \lambda_{reg} \mathcal{L}_{reg} + \lambda_{inter} \mathcal{L}^{inter} + \lambda_{intra} \mathcal{L}^{intra}, \end{aligned} \quad (7)$$

where \mathcal{L}_f represents the classification loss, and \mathcal{L}_{reg} denotes the regression loss, both dedicated to optimizing TL. Conversely, \mathcal{L}^{inter} and \mathcal{L}^{intra} are explicitly employed to enhance the accuracy and discriminative power of HD. Detailed formulations and implementation specifics of each loss term are elaborated in the supplementary materials.

4 Experiments

4.1 Datasets & Experimental Settings

Datasets. We evaluate our method on three widely-used benchmarks: **QVHighlights**, **Charades-STA**, and **TVSum**. QVHighlights [18] is the first benchmark designed for joint evaluation of video temporal grounding and highlight detection. It consists of over 10,000 YouTube videos spanning diverse categories such as lifestyle vlogs, news, and documentaries. Our main experiments were conducted on this dataset. Charades-STA [9] augments the original Charades

Table 1: Performances on QVHighlights *test* and *val* splits. The optimal results are indicated in bold, and the suboptimal results are underlined.

Split	Test							Val						
	TL				HD			TL				HD		
	R1		mAP		≥ Very Good			R1		mAP		≥ Very Good		
Method	@0.5	@0.7	@0.5	@0.75	Avg. mAP	HIT@1		@0.5	@0.7	@0.5	@0.75	Avg. mAP	HIT@1	
MCN [14] <i>ICCV'17</i>	11.4	2.7	24.9	8.2	10.7	-	-	-	-	-	-	-	-	
CAL [7] <i>ICCV'22</i>	25.5	11.5	23.4	7.7	9.9	-	-	-	-	-	-	-	-	
XML+[19] <i>ICCV'20</i>	46.7	33.5	47.9	34.7	34.9	35.4	55.1	-	-	-	-	-	-	
M-DETR [18] <i>NeurIPS'21</i>	52.9	33.0	54.8	29.4	30.7	35.7	55.6	53.9	34.8	-	-	32.2	35.7	55.6
UMT [24] <i>CVPR'22</i>	56.2	41.2	53.4	37.0	36.1	38.2	60.0	60.3	44.3	-	-	38.6	39.9	64.2
UniVTG [23] <i>ICCV'23</i>	58.9	40.9	57.6	35.6	35.5	38.2	61.0	59.7	-	-	-	36.1	38.8	61.8
MH-DETR [38] <i>ICCV'22</i>	60.0	42.4	60.7	38.1	38.3	38.2	60.5	60.8	44.9	60.7	39.6	39.2	38.7	61.7
QD-DETR [26] <i>CVPR'23</i>	62.4	45.0	62.5	39.9	39.9	38.9	62.4	62.7	46.7	62.2	41.8	41.2	39.1	63.0
TR-DETR [31] <i>AAAI'23</i>	64.6	48.9	63.9	<u>43.7</u>	42.6	39.9	63.4	-	-	-	-	-	-	-
TaskWeave [39] <i>CVPR'24</i>	-	-	-	-	-	-	64.2	<u>64.2</u>	50.0	65.3	<u>46.4</u>	<u>45.3</u>	<u>39.2</u>	<u>63.6</u>
UVCOM [36] <i>CVPR'24</i>	<u>63.5</u>	47.4	<u>63.3</u>	42.6	43.1	<u>39.7</u>	64.2	65.1	51.8	-	-	45.7	-	-
MLVTG	64.0	<u>48.3</u>	<u>63.3</u>	43.9	<u>43.0</u>	39.9	<u>63.9</u>	65.1	<u>50.5</u>	<u>63.7</u>	46.8	44.6	40.5	65.2

dataset by adding temporal annotations aligned with natural language. It comprises 9,848 indoor activity videos and 16,128 sentence-moment pairs. It is used to evaluate the model performance on TL. TVSum [30] includes 50 YouTube videos across 10 categories (e.g., DIY tutorials) and is used for HD evaluation.

Evaluation Metrics. We adopt standard evaluation metrics specific to each dataset. For QVHighlights, we follow the official evaluation metric proposed in [19]. For TL, we report Recall@1 at IoU thresholds 0.5 and 0.7, mAP at 0.5 and 0.75, and the average mAP over 0.5–0.95 with a step size of 0.05. For HD, we use mAP and HIT@1, where a clip is counted as correct if its saliency is annotated as *Very Good*. For Charades-STA, we report Recall@1 at IoU 0.5, and 0.7, along with mIoU. For TVSum, we follow the evaluation metric in [30], reporting mAP and Top-5 mAP.

Implementation Details. We concatenate CLIP (ViT-B/32) and SlowFast (R-50) features from pre-segmented video clips at fixed frame rates (0.5/1 FPS), while text features are extracted through the CLIP text encoder. We use $k=4$ vision mamba blocks with $d=1024$ hidden dimensions in the MambaAligner. The LLMRefiner operates on 2056 dimension features extracted from the 20th layer. We use a batch size of 32 and the model is trained for 200 epochs on a single RTX 4090 GPU. Details are provided in the supplementary materials.

4.2 Comparison with Start-of-the-Arts

Joint Temporal Localization and Highlight Detection. Our MLVTG achieves state-of-the-art performance on TL and HD, as shown in Table 1. On

the QVHighlights test set, it outperforms UVCOM by 0.8% in R1@0.7 and achieves the highest mAP@0.75 (43.9) and HD mAP (39.9). Since TR-DETR specifically designs a module utilizing HD to assist the TL on QVHighlights, it performs well. However, more generalized MLVTG outperforms it on the generic TL dataset Charades-STA, as shown in Table 2. On the val set, MLVTG achieves 65.1 R1@0.5 (+0.9% over UVCOM), 50.5 R1@0.7 (+8.6% over QD-DETR), and 46.8 mAP@0.75 (+0.9% over TaskWeave). For HD evaluation, it also reaches 65.2 HIT@1, surpassing UVCOM and QD-DETR by 2.5% and 3.5%.

Temporal Localization. In the TL task, we evaluate MLVTG on the Charades-STA, comparing its performance with advanced temporal localization methods (Table 2). The experiments measure R1@0.3, 0.5, 0.7 and mIoU. MLVTG achieves the best results on R1@0.7 and mIoU, surpassing UVCOM by 2.04% in R1@0.7, highlighting its robustness under strict metrics. Its R1@0.5 (58.3) closely matches UVCOM (59.2), while outperforming detector-based methods like TR-DETR (57.6). Notably, without relying on complex cascading detector designs, MLVTG achieves superior overall performance, indicating balanced localization accuracy and generalization capability.

Table 2: Performances on Charades-STA. The suboptimal results are underlined

Method	Temporal Localization		
	R1		mIoU
	@0.5	@0.7	
CTRL [9]	23.6	8.8	-
MAN [43]	46.5	22.7	-
M-DETR [18]	53.6	31.3	-
VSLNet [44]	54.1	35.2	50.0
UniVTG [23]	58.0	35.6	<u>50.1</u>
QD-DETR [26]	55.5	34.1	-
TR-DETR [31]	57.6	33.5	-
TaskWeave [39]	56.5	33.6	-
UVCOM [36]	<u>59.2</u>	<u>36.6</u>	-
MLVTG	<u>58.3</u>	38.7	50.3

Highlight Detection. On TVSum (Table 3), MLVTG achieves an average F1-score of 80.1, on par with the state-of-the-art CO-AV [21], and excels in fine-grained scenarios. It notably outperforms CO-AV in user-generated content (VU: 85.6, +12.8%) and ads (PR: 87.7, +9.7%). UniVTG uses multiple datasets for training. Even without this, MLVTG remains competitive. MLVTG demonstrates superior generalization capabilities over complex methods like Joint-VA without introducing audio modality, highlighting the advantages of our method.

Table 3: Highlight Detection performance of Top-5 mAP on TVSum. “†” denotes the methods that utilize the audio modality. The suboptimal results are underlined.

Method	Highlight Detection										
	VT	VU	GA	MS	PK	PR	FM	BK	BT	DS	Avg.
Trailer [33]	61.3	54.6	65.7	60.8	59.1	70.1	58.2	64.7	65.6	68.1	62.8
SL-Module [37]	86.5	68.7	74.9	86.2	79.0	63.2	58.9	72.6	78.9	64.0	73.3
PLD-VHD [35]	84.5	80.9	70.3	72.5	76.4	<u>87.2</u>	<u>71.9</u>	74.0	74.4	79.1	77.1
UniVTG [23]	83.9	<u>85.1</u>	89.0	80.1	84.6	81.4	70.9	91.7	73.5	69.3	81.0
MINI-Net† [15]	80.6	68.3	78.2	81.8	78.1	65.8	57.8	75.0	80.2	65.5	73.2
TCG† [40]	<u>85.0</u>	71.4	81.9	78.6	80.2	75.5	71.6	77.3	78.6	68.1	76.8
Joint-VA† [2]	83.7	57.3	78.5	<u>86.1</u>	80.1	69.2	70.0	73.0	97.4	67.5	76.3
CO-AV† [21]	90.8	72.8	<u>84.6</u>	85.0	78.3	78.0	72.8	77.1	<u>89.5</u>	72.3	<u>80.1</u>
MLVTG	83.6	85.6	74.7	75.9	<u>82.4</u>	87.7	64.6	<u>91.6</u>	80.9	73.7	<u>80.1</u>

Table 4: **Ablation Study on Three Benchmarks.** We select the most representative indicators as validation metrics for each task.

Mamba LLM Aligner Refiner	Temporal Localization									Highlight Detection			
	QVHighlights				Charades-STA					QVHighlights		TVSum	
	R1	R5	mIoU	mAP	R1	mIoU	mAP			\geq Very Good	Avg.		
	@0.7	@0.7		@0.75 Avg.	@0.7		@0.75 Avg	HIT@1	mAP				
✗	✗	43.5	59.4	54.7	59.5	39.0	35.6	49.4	38.5	39.0	64.2	39.3	72.7
✓	✗	48.9	66.3	59.1	62.9	42.4	38.7	50.2	41.0	40.4	64.8	40.1	77.1
✗	✓	45.1	61.4	55.8	60.8	39.3	35.4	49.4	38.3	39.4	62.8	38.2	77.7
✓	✓	50.5	66.9	59.9	63.7	44.6	38.7	50.3	41.0	40.8	65.2	40.5	80.1

5 Ablation Study

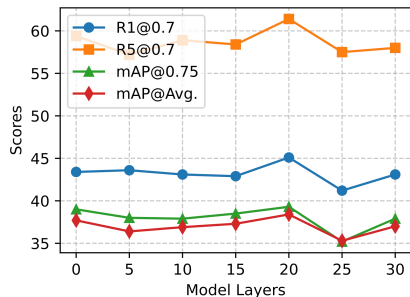
In this section, we conduct ablation studies on three aspects and detailed experimental results are provided in the supplementary materials.

As shown in Table 4, MambaAligner alone significantly boosts TL results—on QVHighlights, R1@0.7 improves by +5.4%, mIoU by +4.4%, and mAP@Avg by +5.3%; on Charades-STA, gains are +3.1%, +0.8%, and +1.4%. LLMRefiner contributes moderate improvements (e.g., +1.6% R1@0.7 on QVHighlights), reflecting its semantic refinement effect. Combining both yields the best TL results, with total gains of +7.0% R1@0.7, +5.2% mIoU, and +5.6% mAP@Avg. On HD, MambaAligner provides +0.8% mAP and +4.4% Avg, LLMRefiner adds minor benefits, and the full model achieves the highest HD performance (+1.2% mAP, +7.4% Avg), confirming their complementarity.

To validate the effectiveness of frozen pre-trained LLM parameters, we conduct experiments on the baseline with different initialization and freezing strategies. All models adopt a single-layer Transformer for fair comparison (Table 5). The baseline achieves 38.4 mAP@Avg. Adding a trainable random initialized

Table 5: **Effectiveness of LLM Pre-trained Parameters.** “—” means no LLM layer. “Rand” means randomly initialized.

LLM Param	Frozen	R1 @0.7	R5 @0.7	mAP @0.75	mAP @Avg.
—	—	43.5	59.4	39.0	37.7
Rand	No	43.6	57.4	37.0	36.7
Rand	Yes	43.3	57.9	38.1	37.1
Yes	No	42.8	57.2	36.9	36.4
Yes	Yes	45.1	61.4	39.3	38.4

Fig. 3: **Effectiveness of LLM Different Layer.**

layer reduces performance by 2.7% (row 2 vs. 1), showing that structural imitation introduces noise. Freezing random initialized layers yields 37.1 (−3.4%, row 3 vs. 5), highlighting the need for pre-trained LLM parameters. Full fine-tuning leads to 36.4 (−5.2%, row 4 vs. 5), confirming that updates disrupt alignment. In contrast, frozen LLMs achieve 45.1 R1@0.7, 38.4 mAP@Avg, and 61.4 R5@0.7, demonstrating better temporal grounding.

Layer-wise analysis reveals that the multi-modal alignment ability of LLMs is highly dependent on layer selection. As shown in Fig 3, using the 20th layer’s frozen parameters yields the best performance. In contrast, higher layer (e.g., 25th) lead to significant degradation, suggesting that excessive abstraction harms visual grounding. Overall, performance shows a parabolic trend across layers, with the range 15–22th forming a “semantic sweet spot” that avoids both syntactic noise from lower layers and semantic oversimplification from higher ones.

6 Visualization

Figure 4 illustrates the cosine similarity heatmap between query and video features. Initially, the alignment between these features is poor, as evidenced by the scattered distribution of similarity scores. Upon introducing MambaAligner, a substantial improvement in the alignment quality between video and textual features is observed. Nevertheless, the presence of spurious regions exhibiting high similarity, particularly in the early video clip due to background distractors, reveals limitations in alignment precision. Subsequent refinement by LLMRefiner markedly enhances alignment accuracy by effectively suppressing noise and concentrating high-similarity regions within the ground-truth interval (63–132 seconds). The visualization explicitly demonstrates the incremental benefit provided by MambaAligner for enhancing alignment and the critical refinement contributed by LLMRefiner for precise localization. Furthermore, Fig. 5 further compares our method MLVTG with the baseline on QVHighlights.

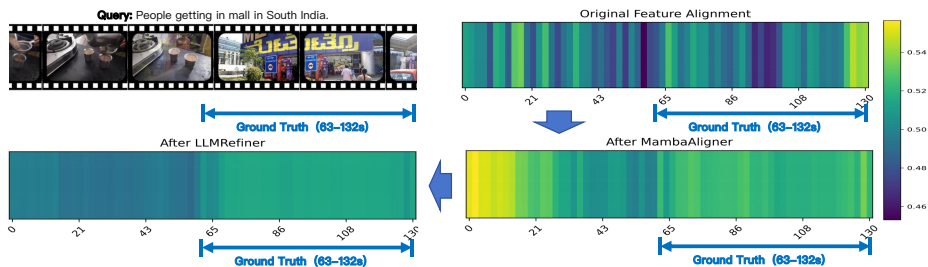


Fig. 4: Feature Alignment Visualization. Darker colors indicate lower similarity.

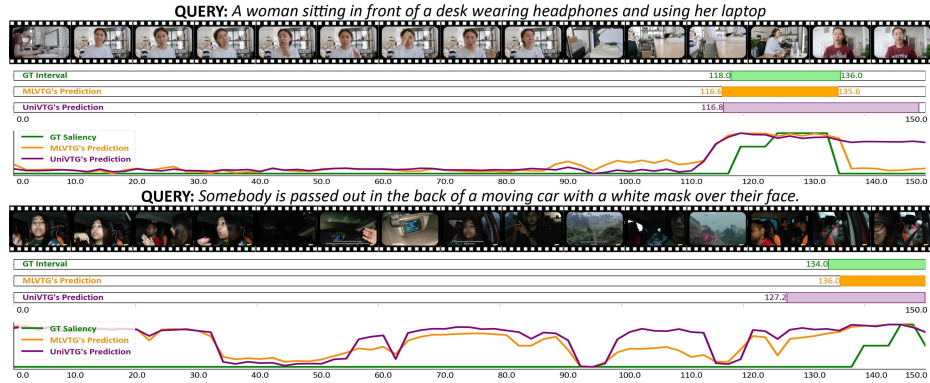


Fig. 5: Visualization of joint temporal localization and highlight detection on QVHighlights.

7 Conclusion

This paper proposes MLVTG, a novel framework for video temporal grounding that combines Mamba and frozen LLM layers for effective multi-modal alignment. Experiments on three benchmarks show that MLVTG outperforms state-of-the-art methods in both temporal localization and highlight detection. Ablation studies further confirm the effectiveness of each component, demonstrating the robustness and superiority of MLVTG. Future work will explore extending MLVTG to incorporate audio modalities for more comprehensive video temporal grounding.

References

1. Arnab, A., Dehghani, M., Heigold, G., Sun, C., Lucic, M., Schmid, C.: Vivit: A video vision transformer. In: ICCV. pp. 6816–6826 (2021)
2. Badamdorj, T., Rochan, M., Wang, Y., Cheng, L.: Joint visual and audio learning for video highlight detection. In: ICCV. pp. 8107–8117 (2021)
3. Beltagy, I., Peters, M.E., Cohan, A.: Longformer: The long-document transformer. CoRR [abs/2004.05150](#) (2020)
4. Carion, N., Massa, F., Synnaeve, G., Usunier, N., Kirillov, A., Zagoruyko, S.: End-to-end object detection with transformers. In: ECCV. vol. 12346, pp. 213–229 (2020)
5. Chen, G., Zheng, Y., Wang, J., Xu, J., Huang, Y., Pan, J., Wang, Y., Wang, Y., Qiao, Y., Lu, T., Wang, L.: Videollm: Modeling video sequence with large language models. CoRR [abs/2305.13292](#) (2023)
6. Driess, D., Xia, F., Sajjadi, M.S.M., Lynch, C., Chowdhery, A., Ichter, B., Wahid, A., Tompson, J., Vuong, Q., Yu, T., Huang, W., Chebotar, Y., Sermanet, P., Duckworth, D., Levine, S., Vanhoucke, V., Hausman, K., Toussaint, M., Greff, K., Zeng, A., Mordatch, I., Florence, P.: Palm-e: An embodied multimodal language model. In: International Conference on Machine Learning, ICML. Proceedings of Machine Learning Research, vol. 202, pp. 8469–8488 (2023)

7. Escorcia, V., Soldan, M., Sivic, J., Ghanem, B., Russell, B.C.: Temporal localization of moments in video collections with natural language. CoRR **abs/1907.12763** (2019)
8. Fu, D.Y., Dao, T., Saab, K.K., Thomas, A.W., Rudra, A., Ré, C.: Hungry hungry hippos: Towards language modeling with state space models. In: ICLR (2023)
9. Gao, J., Sun, C., Yang, Z., Nevatia, R.: TALL: temporal activity localization via language query. In: ICCV. pp. 5277–5285 (2017)
10. Gu, A., Dao, T.: Mamba: Linear-time sequence modeling with selective state spaces. CoRR **abs/2312.00752** (2023)
11. Gu, A., Goel, K., Ré, C.: Efficiently modeling long sequences with structured state spaces. In: ICLR (2022)
12. Gupta, A., Gu, A., Berant, J.: Diagonal state spaces are as effective as structured state spaces. In: NeurIPS (2022)
13. Gygli, M., Song, Y., Cao, L.: Video2gif: Automatic generation of animated gifs from video. In: CVPR. pp. 1001–1009 (2016)
14. Hendricks, L.A., Wang, O., Shechtman, E., Sivic, J., Darrell, T., Russell, B.C.: Localizing moments in video with natural language. In: ICCV. pp. 5804–5813 (2017)
15. Hong, F., Huang, X., Li, W., Zheng, W.: Mini-net: Multiple instance ranking network for video highlight detection. In: ECCV. Lecture Notes in Computer Science, vol. 12358, pp. 345–360 (2020)
16. Huang, B., Wang, X., Chen, H., Song, Z., Zhu, W.: Vtimellm: Empower LLM to grasp video moments. In: CVPR. pp. 14271–14280 (2024)
17. Huh, M., Cheung, B., Wang, T., Isola, P.: Position: The platonic representation hypothesis. In: ICML (2024)
18. Lei, J., Berg, T.L., Bansal, M.: Detecting moments and highlights in videos via natural language queries. In: NeurIPS. pp. 11846–11858 (2021)
19. Lei, J., Yu, L., Berg, T.L., Bansal, M.: TVR: A large-scale dataset for video-subtitle moment retrieval. In: ECCV. Lecture Notes in Computer Science, vol. 12366, pp. 447–463 (2020)
20. Li, K., Li, X., Wang, Y., He, Y., Wang, Y., Wang, L., Qiao, Y.: Videomamba: State space model for efficient video understanding. In: ECCV. Lecture Notes in Computer Science, vol. 15084, pp. 237–255 (2024)
21. Li, S., Zhang, F., Yang, K., Liu, L., Liu, S., Hou, J., Yi, S.: Probing visual-audio representation for video highlight detection via hard-pairs guided contrastive learning. In: BMVC. p. 709 (2022)
22. Liang, A., Jiang, X., Sun, Y., Lu, C.: Bi-mamba4ts: Bidirectional mamba for time series forecasting. CoRR **abs/2404.15772** (2024)
23. Lin, K.Q., Zhang, P., Chen, J., Pramanick, S., Gao, D., Wang, A.J., Yan, R., Shou, M.Z.: Univtg: Towards unified video-language temporal grounding. In: ICCV. pp. 2782–2792 (2023)
24. Liu, Y., Li, S., Wu, Y., Chen, C.W., Shan, Y., Qie, X.: UMT: unified multi-modal transformers for joint video moment retrieval and highlight detection. In: CVPR. pp. 3032–3041 (2022)
25. Liu, Y., Tian, Y., Zhao, Y., Yu, H., Xie, L., Wang, Y., Ye, Q., Jiao, J., Liu, Y.: Vmamba: Visual state space model. In: NeurIPS (2024)
26. Moon, W., Hyun, S., Park, S., Park, D., Heo, J.: Query - dependent video representation for moment retrieval and highlight detection. In: CVPR. pp. 23023–23033 (2023)
27. Pan, Z., Zeng, H., Cao, J., Chen, Y., Zhang, K., Xu, Y.: Mambasci: Efficient mamba-unet for quad-bayer patterned video snapshot compressive imaging. In: NeurIPS (2024)

28. Pang, Z., Xie, Z., Man, Y., Wang, Y.: Frozen transformers in language models are effective visual encoder layers. In: ICLR (2024)
29. Shen, Y., Xiao, L., Chen, J., Du, Q., Ye, Q.: Learning cross-task features with mamba for remote sensing image multitask prediction. *IEEE Trans. Geosci. Remote Sens.* **63**, 1–16 (2025)
30. Song, Y., Vallmitjana, J., Stent, A., Jaimes, A.: Tvsom: Summarizing web videos using titles. In: CVPR. pp. 5179–5187 (2015)
31. Sun, H., Zhou, M., Chen, W., Xie, W.: TR-DETR: task-reciprocal transformer for joint moment retrieval and highlight detection. In: AAAI. pp. 4998–5007 (2024)
32. Sun, M., Farhadi, A., Seitz, S.M.: Ranking domain-specific highlights by analyzing edited videos. In: ECCV. *Lecture Notes in Computer Science*, vol. 8689, pp. 787–802 (2014)
33. Wang, L., Liu, D., Puri, R., Metaxas, D.N.: Learning trailer moments in full-length movies with co-contrastive attention. In: ECCV. *Lecture Notes in Computer Science*, vol. 12363, pp. 300–316 (2020)
34. Wang, Y., Chen, W., Han, X., Lin, X., Zhao, H., Liu, Y., Zhai, B., Yuan, J., You, Q., Yang, H.: Exploring the reasoning abilities of multimodal large language models (mllms): A comprehensive survey on emerging trends in multimodal reasoning. *CoRR* **abs/2401.06805** (2024)
35. Wei, F., Wang, B., Ge, T., Jiang, Y., Li, W., Duan, L.: Learning pixel-level distinctions for video highlight detection. In: CVPR. pp. 3063–3072 (2022)
36. Xiao, Y., Luo, Z., Liu, Y., Ma, Y., Bian, H., Ji, Y., Yang, Y., Li, X.: Bridging the gap: A unified video comprehension framework for moment retrieval and highlight detection. In: CVPR. pp. 18709–18719 (2024)
37. Xu, M., Wang, H., Ni, B., Zhu, R., Sun, Z., Wang, C.: Cross-category video highlight detection via set-based learning. In: ICCV. pp. 7950–7959 (2021)
38. Xu, Y., Sun, Y., Zhai, B., Jia, Y., Du, S.: MH-DETR: video moment and highlight detection with cross-modal transformer. In: IJCNN. pp. 1–8 (2024)
39. Yang, J., Wei, P., Li, H., Ren, Z.: Task-driven exploration: Decoupling and inter-task feedback for joint moment retrieval and highlight detection. In: CVPR. pp. 18308–18318 (2024)
40. Ye, Q., Shen, X., Gao, Y., Wang, Z., Bi, Q., Li, P., Yang, G.: Temporal cue guided video highlight detection with low-rank audio-visual fusion. In: ICCV. pp. 7930–7939 (2021)
41. Ye, Q., Xu, H., Xu, G., Ye, J., Yan, M., Zhou, Y., Wang, J., Hu, A., Shi, P., Shi, Y., Li, C., Xu, Y., Chen, H., Tian, J., Qi, Q., Zhang, J., Huang, F.: mplug-owl: Modularization empowers large language models with multimodality. *CoRR* **abs/2304.14178** (2023)
42. Zeng, W., Jin, S., Liu, W., Qian, C., Luo, P., Ouyang, W., Wang, X.: Not all tokens are equal: Human-centric visual analysis via token clustering transformer. In: CVPR. pp. 11101–11111 (2022)
43. Zhang, D., Dai, X., Wang, X., Wang, Y., Davis, L.S.: MAN: moment alignment network for natural language moment retrieval via iterative graph adjustment. In: CVPR. pp. 1247–1257 (2019)
44. Zhang, H., Sun, A., Jing, W., Zhou, J.T.: Span-based localizing network for natural language video localization. In: ACL. pp. 6543–6554 (2020)
45. Zheng, R., Qi, L., Chen, X., Wang, Y., Wang, K., Qiao, Y., Zhao, H.: Villa: Video reasoning segmentation with large language model. *CoRR* **abs/2407.14500** (2024)
46. Zhu, L., Liao, B., Zhang, Q., Wang, X., Liu, W., Wang, X.: Vision mamba: Efficient visual representation learning with bidirectional state space model. In: ICML (2024)

8 Supplementary Materials

8.1 Training Objectives

TL Prediction Head. The \mathcal{L}_{TL} combines classification loss \mathcal{L}_f and regression loss \mathcal{L}_{reg} :

$$\mathcal{L}_f = -\lambda_f \left(f_i \log \tilde{f}_i + (1 - f_i) \log(1 - \tilde{f}_i) \right), \quad (8)$$

Where $f_i \in \{0, 1\}$ is a binary value indicating whether the i -th clip belongs to the foreground or not, and \tilde{f}_i is the predicted score. For regression, the model predicts temporal offsets $\tilde{d}_i = (\tilde{d}_i^s, \tilde{d}_i^e)$ around reference t_i , defining clip $\tilde{b}_i = [t_i - \tilde{d}_i^s, t_i + \tilde{d}_i^e]$. The loss combines Smooth L1 and gIoU:

$$\mathcal{L}_{reg} = \frac{1}{N_p} \sum_{i: f_i=1} \left[\lambda_{L1} \mathcal{L}_{SmoothL1}(\tilde{d}_i, d_i) + \lambda_{giou} \mathcal{L}_{gIoU}(\tilde{b}_i, b_i) \right], \quad (9)$$

where N_p is the number of foreground clips.

HD Prediction Head. The \mathcal{L}_{HD} is based on dual contrastive learning, combining intra- and inter-video alignment:

$$\mathcal{L}_{HD} = \lambda_{inter} \mathcal{L}^{inter} + \lambda_{intra} \mathcal{L}^{intra}. \quad (10)$$

Intra-video Loss encourages local discrimination by contrasting high-saliency foreground clips with lower-saliency negatives. We randomly sample a foreground clip \mathbf{v}_i with label $f_i = 1$ and saliency score $s_i > 0$ as the positive example, while defining clips with lower saliency scores $\Omega = \{j \mid s_j < s_i\}$ as negative examples. The loss function is given by:

$$\mathcal{L}^{intra} = -\log \frac{\exp(\tilde{s}_i/\tau)}{\exp(\tilde{s}_i/\tau) + \sum_{j \in \Omega} \exp(\tilde{s}_j/\tau)}. \quad (11)$$

Inter-video Loss promotes semantic alignment using cosine similarity to text features across the batch:

$$\mathcal{L}^{inter} = -\log \frac{\exp(\tilde{s}_i/\tau)}{\sum_{k \in B} \exp(\tilde{s}_i^k/\tau)}, \quad (12)$$

where τ is a temperature parameter, and B denotes the batch. Together, these losses help establish a multi-modal semantic bridge via \mathcal{L}^{inter} to ensure alignment between visual features and text; and leveraging \mathcal{L}^{intra} to capture local details for improved localization accuracy.

8.2 Experimental Settings

All feature extractors remain frozen. Training uses multi-task optimization with loss weights: $\lambda_{SmoothL1} = 10$, $\lambda_{giou} = 1$, $\lambda_f = 10$, $\lambda_{intra} = 0.05$, $\lambda_{inter} = 0.1$. Drop path (0.1) is applied to Mamba layers and dropout (0.5) to feature projections. AdamW (lr= 1×10^{-5} , weight decay= 1×10^{-5}) with a 10-epoch warmup is used. A 0.7 NMS threshold is applied for temporal localization.

Table 6: QVHighlights

Base Mamba LLM			Temporal Localization							Highlight Detection		
			R1		R5		mIoU	mAP		mAP	≥ Very Good	
			@0.5	@0.7	@0.5	@0.7		@0.5	@0.75			HIT@1
✓	✗	✗	60.52	43.48	77.61	59.42	54.72	59.51	38.98	37.65	64.19	39.27
✓	✓	✗	65.16	<u>48.90</u>	81.61	<u>66.26</u>	<u>59.12</u>	<u>62.89</u>	<u>44.27</u>	<u>42.39</u>	<u>64.77</u>	<u>40.07</u>
✓	✗	✓	62.58	45.10	78.52	61.35	55.75	60.75	39.30	38.41	62.84	39.21
✓	✓	✓	<u>65.10</u>	50.45	<u>81.48</u>	66.90	59.94	63.70	46.76	44.55	65.23	40.49

8.3 Ablation Study

We conduct comprehensive ablation studies on QVHighlights (joint TL and HD), Charades-STA (TL), and TVSum (HD) datasets, and detailed experimental results are shown in Tables 6, Table 7 and Table 8.

Table 7: Charades-STA

Base Mamba LLM			Temporal Localization						
			R1			mIoU	mAP		mAP
			@0.3	@0.5	@0.7		@0.5	@0.75	
✓	✗	✗	69.60	<u>57.93</u>	35.62	49.43	67.98	38.46	38.93
✓	✓	✗	69.27	57.74	<u>38.68</u>	<u>50.16</u>	68.29	<u>40.96</u>	<u>40.39</u>
✓	✗	✓	69.68	57.42	35.35	49.43	<u>68.57</u>	38.31	39.38
✓	✓	✓	<u>69.60</u>	58.31	38.68	50.34	68.71	40.97	40.80

When replacing the transformer in UniVTG with Mamba architecture, we observe consistent performance gains across all tasks. Specifically, on QVHighlights, Mamba brings +4.64% R1@0.5 and +6.84% R5@0.7 improvements in VTG, along with +3.38% mAP@0.5 in HD. The LLM semantic optimizer demonstrates complementary benefits, particularly enhancing temporal localization precision with +1.06% R1@0.7 improvement on QVHighlights. The full model achieves state-of-the-art performance through synergistic effects: 50.45% R1@0.7 (+6.97% absolute) on QVHighlights VTG, 58.31% R1@0.5 on Charades-STA, and 80.08% average score on TVSum HD. Notably, Mamba shows stronger impact on long-sequence modeling (QVHighlights R5@0.7 +6.84%), while LLM excels in semantic-aware localization (TVSum BK: 91.61% vs baseline 83.23%). This validates our architectural design’s effectiveness in multimodal alignment.

Table 8: TVSum

Base Mamba LLM		Highlight Detection											
		VT	VU	GA	MS	PK	PR	FM	BK	BT	DS	Avg.	
✓	✗	✗	84.66	69.31	82.59	78.08	72.92	76.51	40.88	83.23	69.70	69.05	72.69
✓	✓	✗	75.17	85.42	88.29	73.55	78.21	72.42	48.48	88.39	86.83	74.08	77.08
✓	✗	✓	81.67	92.46	89.52	75.12	79.10	67.80	64.36	84.46	69.85	72.90	77.72
✓	✓	✓	83.56	85.60	74.72	75.95	82.42	87.71	64.63	91.61	80.85	73.71	80.08

8.4 Analysis of LLMRefiner Architecture

Table 9 shows that when connecting the transformer-based frozen large language model (LLaMA) specific layer after MambaAligner, performance degraded significantly. We hypothesize that the differing model architectures disrupted the representations learned by MambaAligner, which led to this outcome. So we design the mamba-based LLMRefiner.

Table 9: **The Effectiveness of LLaMA Layer.** The 1st row shows the results on QVHighlights Val using only the MambaAligner module.

Layer	R1		R5		mAP		
	@0.5	@0.7	@0.5	@0.7	@0.5	@0.75	@Avg.
-	65.16	48.9	81.61	66.26	62.89	44.27	42.39
5th	61.81	44.84	79.23	61.48	60.09	40.66	38.81
10th	65.10	46.97	82.58	65.29	62.94	42.79	40.74
15th	64.19	46.19	82.39	63.29	62.74	40.96	40.15
20th	62.97	41.55	81.48	62.06	61.53	38.43	37.84
25th	61.16	42.13	82.65	63.42	60.87	38.7	37.59
30th	61.29	41.81	81.35	62.26	60.22	37.7	36.87